Discovering Multi-Layer Films for Electromagnetic Interference Shielding and Passive Cooling with Multi-Objective Active Learning

Mingxuan Li
University of Pittsburgh
Pittsburgh, PA 15261, USA
mil152@pitt.edu

Jungtaek Kim
University of Pittsburgh
Pittsburgh, PA 15261, USA
jungtaek.kim@pitt.edu

Paul W. Leu
University of Pittsburgh
Pittsburgh, PA 15261, USA
pleu@pitt.edu

Abstract

This work presents a novel framework utilizing multi-objective optimization for the design of photonic structures that concurrently address electromagnetic interference shielding and passive cooling. By exploring different multi layer structures, the study illustrates how increasing complexity correlates with enhanced performance but also raises fabrication challenges. Specifically, an eight-layer configuration demonstrates an ability to achieve both substantial electromagnetic interference shielding effectiveness of 61.77 dB and passive cooling power of 59.61 W/m^2. The ongoing experimental validations of these structures point towards promising applications in enhancing the sustainability and safety of data centers.

1 Introduction

Electromagnetic interference (EMI) shielding is crucial for ensuring data integrity, computation accuracy, and reliable communication. It protects electronic systems from external interference that could disrupt operations and prevents the leakage of electromagnetic (EM) emissions, which could compromise security and performance [13, 8]. On the other hand, proper thermal management is vital for sustaining the performance and reliability of electronic equipment [3]. Cooling systems for high-performance compute machines are essential to maintaining optimal operating temperatures and preventing overheating, and guaranteeing continuous operation. As the demand for computational power increases and the devices become densely packed, especially with the rise of cloud computing, artificial intelligence, and large-scale data processing, the need for advanced solutions in EMI shielding and thermal management is becoming significantly critical, particularly in data centers [6].

Traditionally, EMI shielding has been achieved using conductive metals in the form of foils and sheets to shield enclosures, cables, and entire rooms. Recently, new EMI shielding approaches have emerged, such as the development of high-performance metal meshes [11, 14] and thin films [4, 9, 10, 7]. For cooling, air conditioning and chilled water systems are standard. However, recent research is exploring novel liquid cooling techniques, including microfluidics, immersion cooling, and direct liquid cooling, along with advanced materials like diamond-copper nanocomposites and phase-change materials. Innovations in cooling have also included making use of the environment, for example by locating data centers or high-performance compute clusters near naturally occurring cold water sources or lower ambient temperatures.

In this paper, we explore a novel approach to EMI shielding and cooling through the use of multilayer thin films that incorporate metal layers for EMI shielding and leverage thermal radiation to the coldness of space for passive cooling [2, 12]. Utilizing a non-dominated sorting genetic algorithm II (NSGA-II) for multi-objective optimization and qNEHVI-based Bayesian optimization (BO), we identify optimal configurations that achieve both EM protection and effective thermal management.

This study addresses the urgent need for dual-functional materials in data centers and also contributes to the broader understanding of integrating photonic design with machine learning techniques to enhance operational efficiencies in critical infrastructures.

2 Methodology

Numerical Simulation. The transfer matrix method is used for modeling the propagation of EM waves through the multilayered media [1]. Each layer is defined by its thickness and refractive indices over wavelengths. We use Ansys Optics for these simulations.

Optimization Problem. To find the optimal configuration of thicknesses $\mathbf{t}$ and materials $\mathbf{m}$ that maximizes the objective functions, we define an optimization problem using a multi-objective optimization framework. This can be described as follows: Given a multilayer system with L layers, each layer l can be described by its thickness t_l and material type m_l. The objective is to optimize a vector of thicknesses $\mathbf{t} = [t_1, t_2, \ldots, t_L]$ and a vector of material types $\mathbf{m} = [m_1, m_2, \ldots, m_L]$ to maximize two conflicting objectives, which are the EMI shielding efficiency (SE), $f_{\text{EMI}}(\mathbf{t}, \mathbf{m})$, and the net cooling power, $P_{\text{cooling}}(\mathbf{t}, \mathbf{m})$.

The optimization problem can be formulated as follows:

$$\arg\max_{\mathbf{t}, \mathbf{m}} \ (f_{\text{EMI}}(\mathbf{t}, \mathbf{m}), \ P_{\text{cooling}}(\mathbf{t}, \mathbf{m})). \tag{1}$$

The SE, f_{EMI}, is derived from a physical simulator using the stackrt function. In this simulation, the refractive indices of the materials are utilized, and the transfer matrix method (TMM) is applied to compute the scattering parameters. f_{EMI} is then calculated based on the scattering parameters obtained from the simulation. Specifically, f_{EMI} is computed using the formula:

$$f_{\text{EMI}}(\mathbf{t}, \mathbf{m}) = -10 \log_{10}\left(\frac{t_s + t_p}{2}\right), \tag{2}$$

where T_s and T_p are their transmittances for s- and p-polarized EM waves, respectively.

The net cooling power, P_{cool}, and its components are quantified through several integral equations, accounting for radiant, solar, and atmospheric thermal interactions:

$$P_{\text{cool}}(T) = P_{\text{rad}}(T_s) - P_{\text{sun}}(T_{\text{sun}}) - P_{\text{atm}}(T_{\text{amb}}). \tag{3}$$

The radiative power, P_{rad}, is calculated as an integral of the blackbody spectral emission modulated by the emissivity of the surface material, over all wavelengths and angles:

$$P_{\text{rad}}(T_s) = A \int_0^\infty \int \cos\theta \, I_{bb}(\lambda, T_s) \, \epsilon_s(\lambda, \theta) \, d\Omega \, d\lambda, \tag{4}$$

where $\int \cos\theta d\Omega$ denotes integration over a hemisphere, $\epsilon_s(\lambda, \theta)$ represents the emissivity dependent on wavelength and angle, and $I_{bb}(T, \lambda)$ is given by Planck's law:

$$I_{bb}(T, \lambda) = \frac{2hc^2}{\lambda^5}\left[\frac{1}{e^{(hc/(\lambda k_B T))} - 1}\right]. \tag{5}$$

Note that $h = 6.626 \times 10^{-34}\,\text{J} \cdot \text{s}$ is the Planck constant, $k_B = 1.381 \times 10^{-23}$ J/K is the Boltzmann constant, and $c = 2.988 \times 10^8$ m/s is the speed of light. The downward thermal radiation from the atmosphere is described as below:

$$P_{\text{atm}}(T_{\text{amb}}) = A \int_0^\infty \int \cos\theta I_{bb}(\lambda, T_{\text{amb}})\epsilon_{\text{atm}}(\lambda, \theta)\epsilon_s(\lambda, \theta)d\Omega d\lambda. \tag{6}$$

The emissivity of the atmosphere, $\epsilon_{\text{atm}}(\lambda, \theta)$, accounts for both wavelength and angular dependencies. The power absorbed from solar radiation is determined by the following:

$$P_{\text{sun}}(T_{\text{sun}}) = A \int_0^\infty \epsilon_s(\lambda, \theta_{\text{sun}})I_{\text{sun}}(\lambda)d\lambda. \tag{7}$$

This captures the interaction of the system with solar irradiance, integrating over all solar wavelengths.

Constraints. Each layer's thickness t_l must be within the feasible range defined by the physical properties and manufacturing capabilities. Considering the capability of standard clean room fabrication, the limits have been set as $t_{min} = 15$ nm and $t_{max} = 400$ nm: $t_{min} \leq t_l \leq t_{max}$, for all $l = 1, 2, \ldots, L$. Each layer's material m_l must be selected from a predefined set of materials $\mathcal{M}$ which is detailed in Appendices: $m_l \in \mathcal{M}$, for all $l = 1, 2, \ldots, L$.

3 Physical Background

As illustrated in Figure 1a, the layout of layered materials with chosen thicknesses enables the tuning of the emission waveband. In addition to the optical properties, infrared (IR) vibrations of the materials play a significant role in determining the thermal radiation characteristics of the photonic structures. In our simulations, the emissivity $\epsilon_s(\lambda, \theta)$ inherently accounts for the material's phonon interactions within the mid-

Figure 1: (a) Bragg Reflector structure, (b) Schematic of EMI protecting passive cooling.

infrared range (4 μm to 20 μm). The refractive indices used in the transfer matrix method incorporate contributions from both electronic transitions and lattice vibrations, ensuring that the IR vibrational modes are effectively modeled. This comprehensive treatment allows for accurate simulation of passive cooling power by capturing the essential thermal emission processes governed by IR vibrations. This is done by designing the structure to support specific waveband emissions through the selective transmission and reflection of light. Such configurations typically consist of alternating layers of materials that possess different refractive indices, allowing for the targeted manipulation of light paths through the structure. This method not only enhances reflectivity through constructive interference but also optimizes the radiative cooling process by maximizing the thermal insulation capabilities of the structure. By adjusting the material properties and layer thicknesses, these photonic structures can be finely tuned to optimize energy efficiency and thermal management in various applications [5].

Figure 1b shows the use of photonic structures in EMI-protecting passive cooling systems, which may have applications to data centers. The diagram demonstrates how EMI is managed and how photonic technologies contribute to cooling by reflecting solar radiation while also managing internal heat dissipation.

4 Experimental Results

Bayesian Optimization. BO is employed to explore the design space of multi-layer photonic structures with the goal of optimizing both SE and passive cooling power. Each experiment involved configurations with 4, 6, 8 layers, employing a mixture of materials to determine the optimal thickness and material composition that maximizes performance metrics. The optimization was performed using a Bayesian framework where a mixed variable model was employed, consisting of both categorical variables representing material choices and continuous variables denoting layer thicknesses. The initial data for the optimization were generated using Sobol sequences to ensure a diverse and well-distributed starting point in the design space.
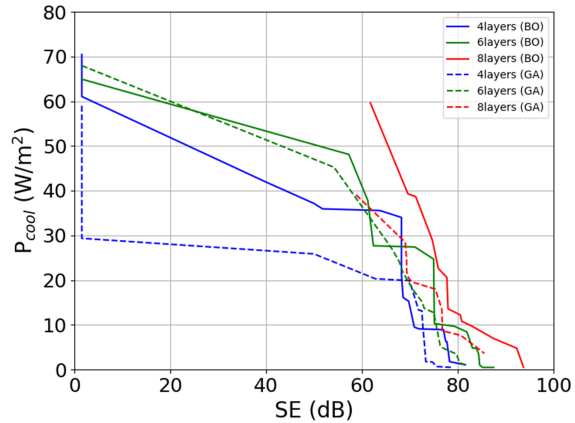
Figure 2: Pareto Frontier for Bayesian Optimization and Genetic Algorithm on 4, 6, 8 layer structures

Each set of experiments involved 1000 iterations, where the design configurations were evaluated using a FDTD solver and custom script to simulate the EM and thermal behavior of each pro-
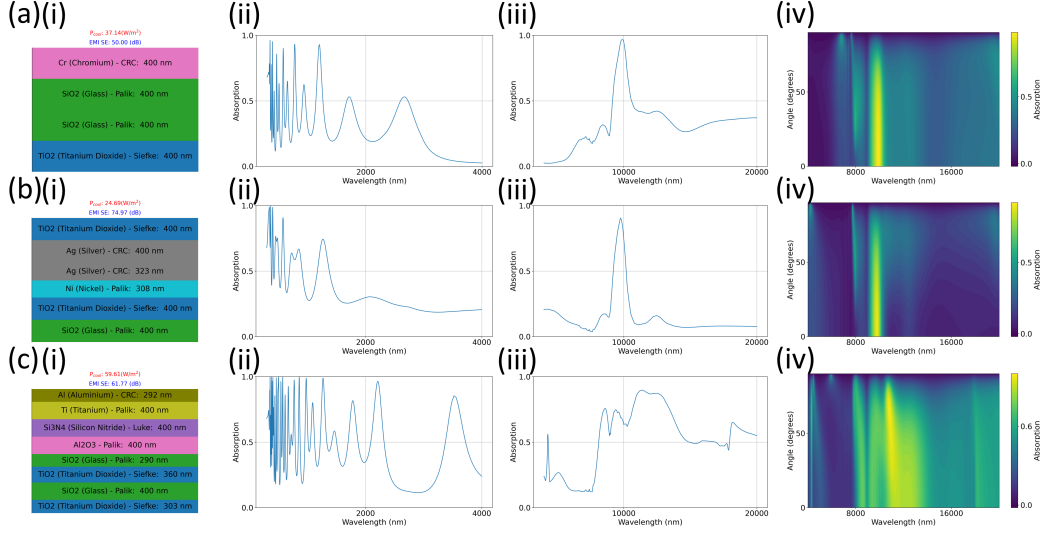
Figure 3: (a)-(c) Structure examples with 4, 6, and 8 layers selected from the Pareto Frontier. Panels (i) show the selected structures, display the absorption spectra from (ii) 300 nm to 4 μm, (iii) 4 μm to 20 μm, and (iv) angular-dependent absorption spectra in the mid-infrared range of 4 μm to 20 μm.

posed design. The solver calculated SE and P_{cool} based on the material properties and geometrical configuration of each layer setup.

Genetic Algorithm.   We employed genetic algorithm (GA) to explore the potential of evolutionary strategies in the design of photonic structures. GA was specifically tailored to handle both categorical variables representing material selections and continuous variables for the thickness of each layer. The optimization process began with the generation of an initial population, derived from a diverse sampling of the predefined material library and permissible thickness range. Each individual in the population represented a potential solution encoded as a combination of material types and layer thicknesses. To maintain genetic diversity and facilitate effective exploration of the design space, the algorithm utilized custom mutation functions. These functions were designed to adjust the material type and layer thickness within defined bounds, ensuring that the mutations led to feasible and varied design proposals. The selection mechanism implemented in the GA was based on the principles of NSGA-II. It systematically ranked individuals based on optimal trade-offs between SE and P_{cool}.

Pareto Frontier Comparison.   As illustrated in Figure 2, BO consistently outperforms GA across all considered layer configurations—4, 6, and 8 layers—demonstrated by its ability to extend the hypervolume of the Pareto frontier. This is particularly evident in the broader spans of both SE and P_{cool} achieved by BO, signifying a superior balance of EMI shielding and passive cooling capabilities. This comparison highlights the advantage of employing Bayesian Optimization for complex multi-objective optimization tasks in photonic design, offering insights into achieving optimal structural configurations with greater robustness and higher performance metrics.

5   Conclusion and Future Work

In this study, we presented a comprehensive framework for multi-objective optimization aimed at designing photonic structures that both mitigate EMI and enhance passive cooling. The exploration of structures with 4, 6, 8, and 10 layers reveals that configurations with more layers, while more sophisticated and possessing larger hypervolumes of objectives are more challenging to fabricate. Notably, the eight-layer structure demonstrated the capability to achieve a passive cooling power of 59.61 W/m^2 and an SE of 61.77 dB, illustrating its efficiency in shielding EM waves and dissipating heat. The methodologies and findings from this study will lay a solid foundation for future work in the field of photonic materials science, particularly in applications aimed at making energy systems more efficient and environmentally friendly.

Acknowledgments and Disclosure of Funding

References

[1] M. Born and E. Wolf. *Principles of optics: electromagnetic theory of propagation, interference and diffraction of light*. Cambridge University Press, 1999.

[2] S. Fan and W. Li. Photonics and thermodynamics concepts in radiative cooling. *Nature Photonics*, 16(3):182–190, 2022.

[3] Y. Fulpagare and A. Bhargav. Advances in data center thermal management. *Renewable and Sustainable Energy Reviews*, 43:981–996, 2015.

[4] A. J. Galante, B. C. Pilsbury, M. Li, M. LeMieux, Q. Liu, and P. W. Leu. Achieving highly conductive, stretchable, and washable fabric from reactive silver ink and increased interfacial adhesion. *ACS Applied Polymer Materials*, 4(7):5253–5260, 2022.

[5] S. Y. Jeong, C. Y. Tso, J. Ha, Y. M. Wong, C. Y. Chao, B. Huang, and H. Qiu. Field investigation of a photonic multi-layered tio2 passive radiative cooler in sub-tropical climate. *Renewable Energy*, 146:44–55, 2020.

[6] K. Kant. Data center evolution: A tutorial on state of the art, issues, and challenges. *Computer Networks*, 53(17):2939–2965, 2009.

[7] J. Kim, M. Li, O. Hinder, and P. Leu. Datasets and benchmarks for nanophotonic structure and parametric design simulations. *Advances in Neural Information Processing Systems*, 36, 2024.

[8] M. G. Kuhn. Electromagnetic eavesdropping risks of flat-panel displays. In *International Workshop on Privacy Enhancing Technologies*, pages 88–107. Springer, 2004.

[9] M. Li, S. Sinha, S. Hannani, S. B. Walker, M. LeMieux, and P. W. Leu. Ink-coated silver films on pet for flexible, high performance electromagnetic interference shielding and joule heating. *ACS Applied Electronic Materials*, 5(1):173–180, 2022.

[10] M. Li, M. Zarei, A. J. Galante, B. Pilsbury, S. B. Walker, M. LeMieux, and P. W. Leu. Stretchable and wash durable reactive silver ink coatings for electromagnetic interference shielding, joule heating, and strain sensing textiles. *Progress in Organic Coatings*, 179:107506, 2023.

[11] M. Li, M. Zarei, K. Mohammadi, S. B. Walker, M. LeMieux, and P. W. Leu. Silver meshes for record-performance transparent electromagnetic interference shielding. *ACS Applied Materials & Interfaces*, 15(25):30591–30599, 2023.

[12] A. P. Raman, M. A. Anoma, L. Zhu, E. Rephaeli, and S. Fan. Passive radiative cooling below ambient air temperature under direct sunlight. *Nature*, 515(7528):540–544, 2014.

[13] S. Saadat. The impact of emi on security access control in datacenter data halls. In *2023 IEEE 22nd International Conference on Trust, Security and Privacy in Computing and Communications (TrustCom)*, pages 1400–1407. IEEE, 2023.

[14] M. Zarei, M. Li, E. E. Medvedeva, S. Sharma, J. Kim, Z. Shao, S. B. Walker, M. LeMieux, Q. Liu, and P. W. Leu. Flexible embedded metal meshes by sputter-free crack lithography for transparent electrodes and electromagnetic interference shielding. *ACS Applied Materials & Interfaces*, 16(5):6382–6393, 2024.

A   Refractive Indices of Materials
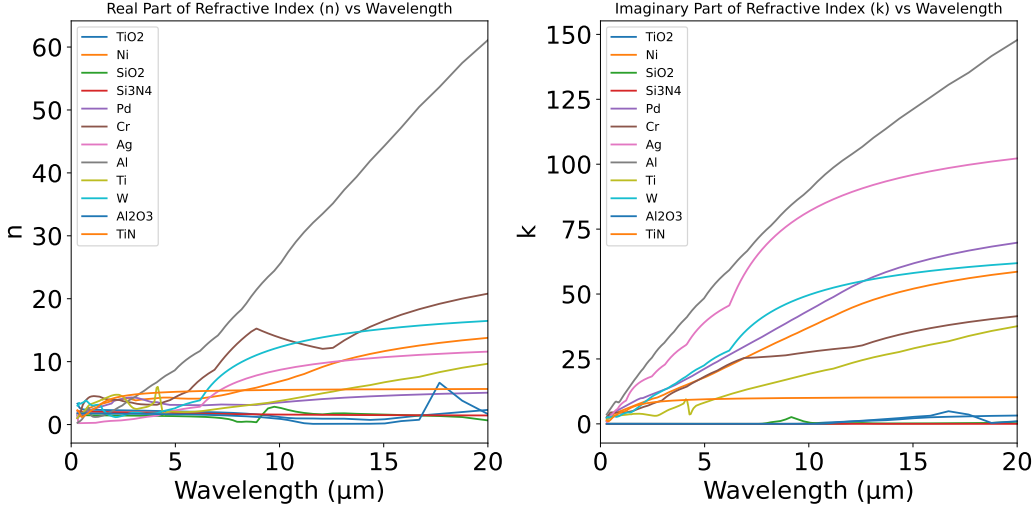
Figure 4: Refractive indices (n, k) of materials explored

Figure 4 presents the refractive indices of the materials explored in this work.

B   Implementation of Optimization

Bayesian Optimization (BO).   Bayesian Optimization (BO) is employed to efficiently explore the high-dimensional design space of multi-layer photonic structures, aiming to optimize both Shielding Effectiveness (SE) and passive cooling power (P_{cool}). Our BO implementation utilizes a Gaussian Process (GP) surrogate model with a Matérn 5/2 kernel, which balances flexibility and smoothness in modeling complex functions. Hyperparameters of the GP are optimized via maximum likelihood estimation during the initial iterations. The acquisition function employed is the q-Non-dominated Expected Hypervolume Improvement (qNEHVI), selected for its effectiveness in multi-objective optimization by directly targeting improvements in the Pareto front hypervolume.

To initialize the BO process, we generate an initial dataset of design configurations using Sobol sequences, ensuring a diverse and well-distributed sampling of the design space. Each BO experiment comprises 1000 iterations. In each iteration, the BO framework proposes new design configurations based on the acquisition function, which are then evaluated using a Finite-Difference Time-Domain (FDTD) solver coupled with custom simulation scripts. The solver calculates SE and P_{cool} based on the material properties and geometrical configurations of each layer setup, providing feedback to update the surrogate model.

Genetic Algorithms (GA).   Genetic Algorithms (GA) are utilized to explore evolutionary strategies in designing photonic structures with enhanced EMI shielding and radiative cooling capabilities. Our GA implementation follows the NSGA-II framework, renowned for its efficiency in handling multi-objective optimization problems. Key parameters for the GA include a population size of 100 individuals, 10 generations, a crossover rate of 0.9, and a mutation rate of 0.1. The selection mechanism is based on binary tournament selection, prioritizing Pareto dominance and maintaining population diversity through crowding distance.

Each individual in the population represents a potential solution, encoded as a combination of material types (categorical variables) and layer thicknesses (continuous variables). Custom mutation functions are developed to adjust both material types and layer thicknesses within feasible ranges, ensuring valid and diverse design proposals. Crossover operations employ uniform crossover, facilitating the exchange of material and thickness information between parent individuals to create offspring with mixed traits. The GA iteratively improves the population by selecting individuals based on Pareto

dominance and diversity measures, effectively converging towards optimal trade-offs between SE and P_{cool}.

C Experimental Data
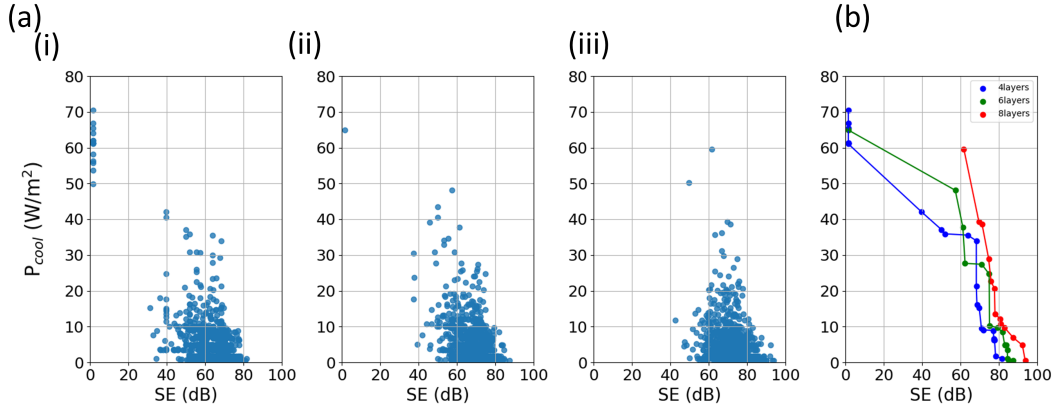
Figure 5: (a)(i)-(iii) BO with 1000 runs of experiment data points for 4, 6, 8 layers, (b) Pareto frontier of structures with 4, 6, 8 layers.

Figure 5 showcases the distribution of experiment data points across different layer configurations (panels a) and the derived multi-objective Pareto frontiers (panel b). Panels a to d represent the scatter of the 1000 runs for structures with 4, 6, 8 layers, respectively, showing the diversity in performance outcomes. Panel b illustrates the Pareto frontiers, highlighting optimal trade-offs between SE and P_{cool} that were achieved across different layer counts. The blue line representing 4 layers demonstrates a steep drop in passive cooling power (P_{cool}) as SE increases, signifying a pronounced trade-off in simpler structures. With 8 layers, depicted by the red line, this trend continues, indicating that additional layers may help moderate the trade-off between SE and P_{cool}. These results demonstrate the effectiveness of Bayesian Optimization in navigating complex design spaces with multiple objectives and constraints, providing a robust method for discovering high-performance designs in the field of photonic radiative cooling and EMI shielding.
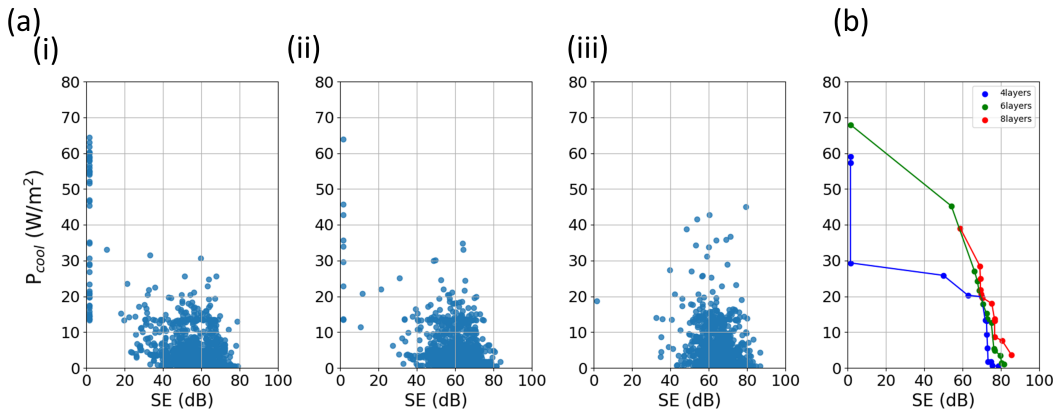
Figure 6: (a)(i)-(iii) Genetic Algorithm 1000 runs of experiment data points for 4, 6, 8 layers (b) EMI SE and Pcool multi-objective Pareto Frontier of 4, 6, 8 layers structures.

Figure 6 provides the experimental results. Panels (a) display the distribution of the 1000 experimental runs for each of the layer configurations, illustrating the broad range of performance outcomes encountered across the design space. Panel (b) depicts the multi-objective Pareto frontiers, which capture the best trade-offs achieved between SE and P_{cool} for each layer configuration. This result showcases the optimal designs and underscores the capability of the GA to effectively navigate and

7
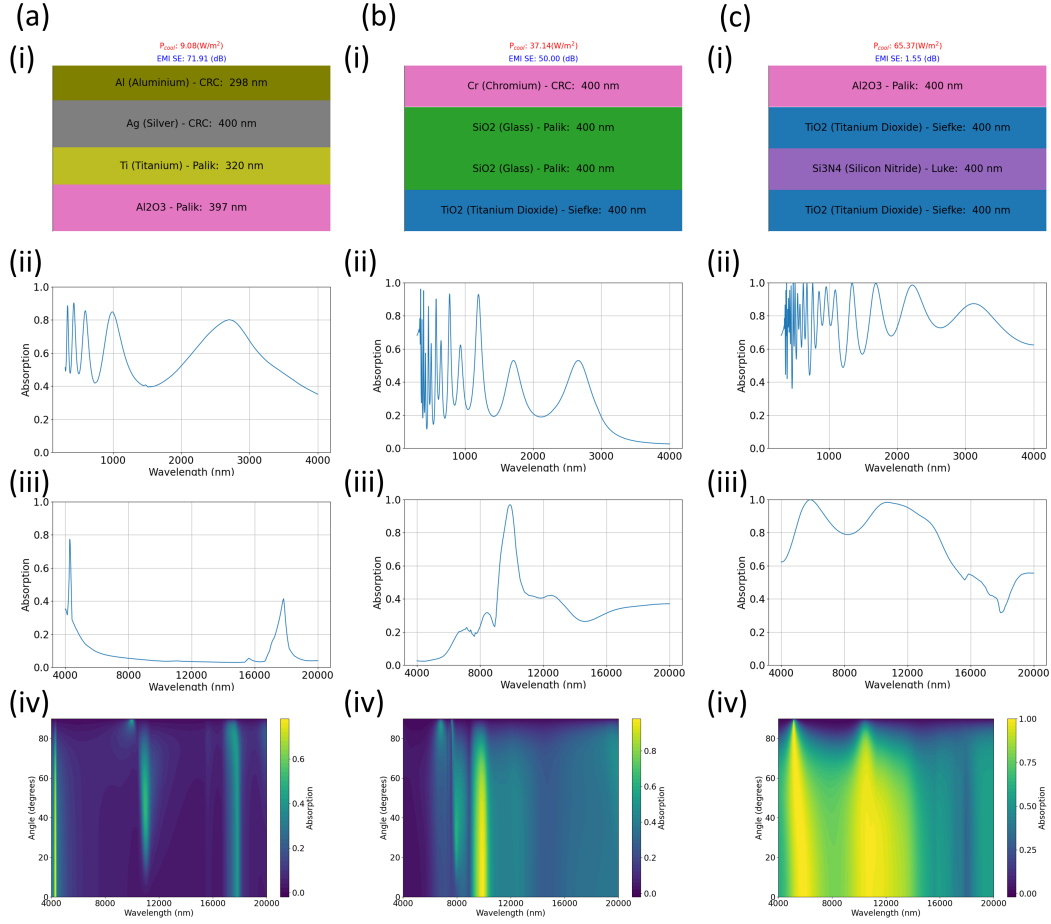
Figure 7: (a)-(c) Selected structures on Pareto Frontier of 4-layer structures showcasing (i) the layer configuration, (ii) Near Infrared Absorption spectrum (300nm-4μm), (iii) Mid Infrared Absorption spectrum (4μm-20μm), and (iv) Angle dependency of the Mid Infrared Absorption spectrum.

exploit complex design spaces, making it a powerful tool in the quest for high-performance photonic structures in applications demanding precise control over EM and thermal properties.

D More Example Structures and Spectra on Pareto Frontier

This section examines the spectral characteristics and physical configurations of photonic multilayer structures that have been optimized to demonstrate effective trade-offs between EMI shielding effectiveness (SE) and passive cooling power (P_{cool}). Detailed analyses were conducted for structures with varying layer counts: 4, 6, 8, and 10 layers. Each structure's performance was evaluated based on its position on the Pareto frontier, indicative of optimal trade-offs between SE and P_{cool}.

In the analysis of photonic multilayer structures, each set of layers was examined through four key components: structural visualization which illustrates each structure's layer composition and thickness for insights into their physical construction; near-infrared absorption spectrum analysis from 300 nm to 4 μm to understand interactions with near-infrared light; mid-infrared absorption spectrum evaluations from 4 μm to 20 μm crucial for assessing thermal radiation management capabilities; and angle dependency analysis to determine how absorption varies with the angle of incidence in the mid-infrared range, reflecting operational performance under various conditions. These analyses utilized FDTD simulations that detailed EM behavior across different spectral ranges for both polarized and unpolarized light. The process included selecting diverse structures using k-means clustering on SE values to ensure broad representation across the Pareto frontier, simulating

8
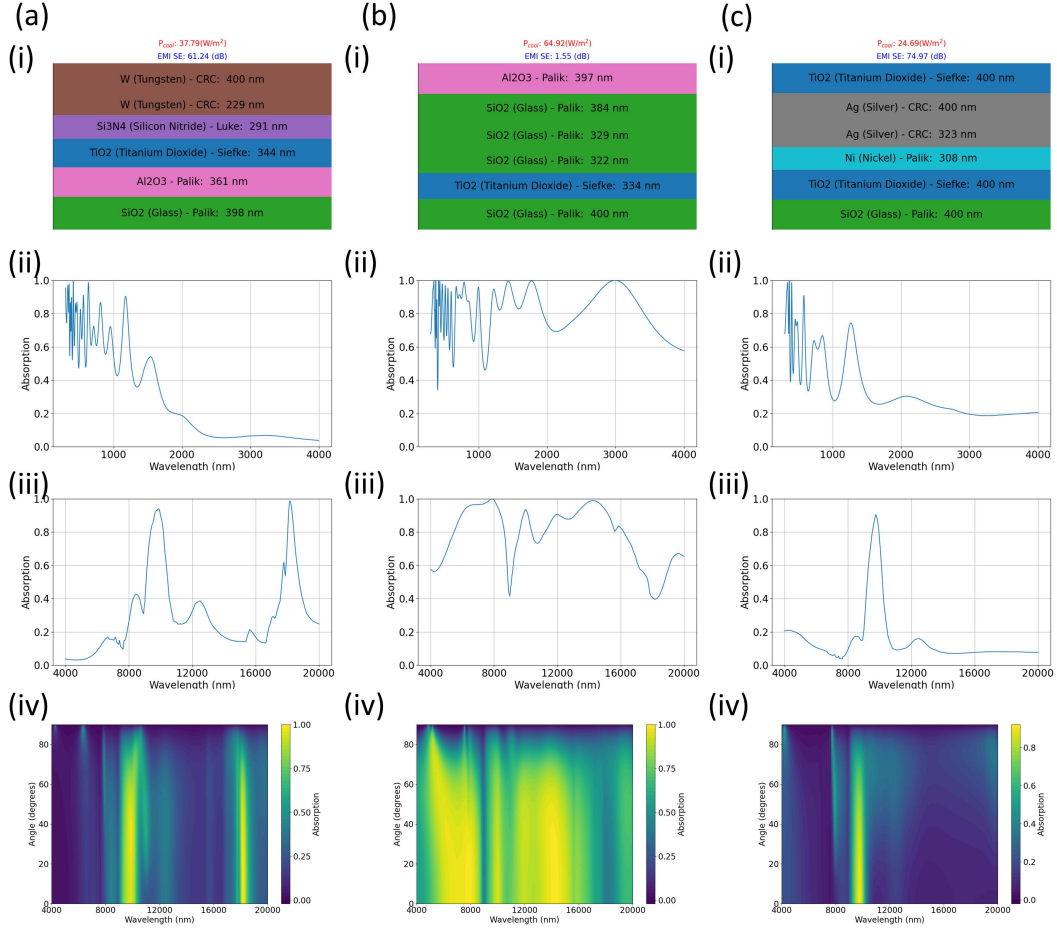
Figure 8: (a)-(c) Selected structures on Pareto Frontier of 6-layer structures showcasing (i) the layer configuration, (ii) Near Infrared Absorption spectrum (300nm-4μm), (iii) Mid Infrared Absorption spectrum (4μm-20μm), and (iv) Angle dependency of the Mid Infrared Absorption spectrum.

the spectral response to derive detailed absorption profiles, and generating plots to correlate structural configurations with optical properties. The practical implications of these studies aim to inform the design and optimization of photonic structures for applications such as solar energy utilization and electronic thermal management, linking structural configurations with spectral behavior to aid in material selection and layer design. The results highlight the utility of advanced computational analyses in materials science, showcasing the complex relationship between a structure's physical configuration and its EM properties, and laying a foundation for further optimization of photonic multilayer structures for targeted industrial applications.
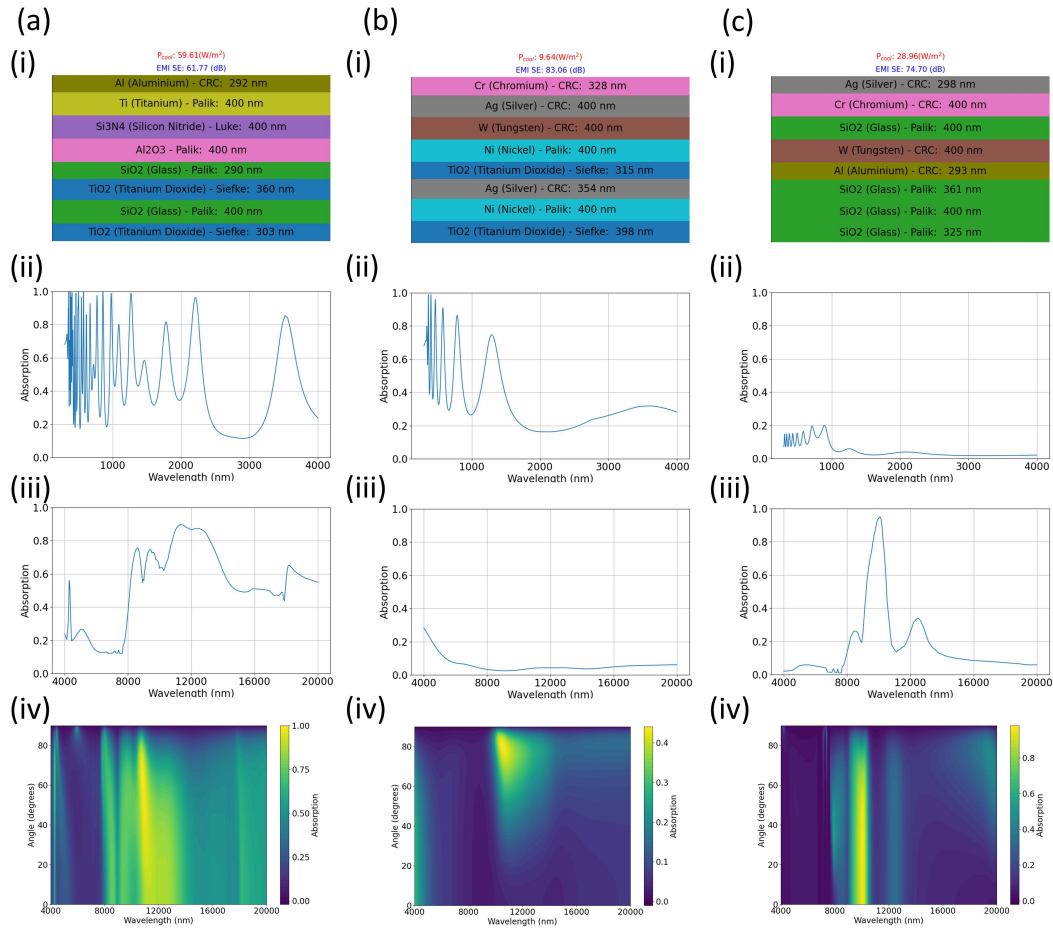
Figure 9: (a)-(c) Selected structures on Pareto Frontier of 8-layer structures showcasing (i) the layer configuration, (ii) Near Infrared Absorption spectrum (300nm-4μm), (iii) Mid Infrared Absorption spectrum (4μm-20μm), and (iv) Angle dependency of the Mid Infrared Absorption spectrum.